

JGR Atmospheres

RESEARCH ARTICLE

10.1029/2020JD033628

Key Points:

- The strong cooking organic aerosol (COA) sources are evidenced by two apparent peaks at lunch time and dinner time in the diurnal cycles
- COA plays a critical role in altering aerosols hygroscopicity in populated urban atmosphere
- The decrease of water uptake capacity of aerosols caused by COA will reduce the aerosol cloud condensation nuclei (CCN) activity greatly

Supporting Information:

Supporting Information may be found in the online version of this article.

Correspondence to:

F. Zhang,
fang.zhang@bnu.edu.cn

Citation:

Liu, J., Zhang, F., Xu, W., Chen, L., Ren, J., Jiang, S., et al. (2021). A large impact of cooking organic aerosol (COA) on particle hygroscopicity and CCN activity in urban atmosphere. *Journal of Geophysical Research: Atmospheres*, 126, e2020JD033628. <https://doi.org/10.1029/2020JD033628>

Received 3 AUG 2020
 Accepted 23 MAR 2021

A Large Impact of Cooking Organic Aerosol (COA) on Particle Hygroscopicity and CCN Activity in Urban Atmosphere

Jieyao Liu¹, Fang Zhang¹ , Weiqi Xu², Lu Chen¹, Jingye Ren¹, Sihui Jiang¹, Yele Sun² , and Zhanqing Li³ 

¹College of Global Change and Earth System Science, Beijing Normal University, Beijing, China, ²State Key Laboratory of Atmospheric Boundary Layer Physics and Atmospheric Chemistry, Institute of Atmospheric Physics, Chinese Academy of Sciences, Beijing, China, ³Earth System Science Interdisciplinary Center and Department of Atmospheric and Oceanic Science, University of Maryland, College Park, MD, USA

Abstract Cooking organic aerosol (COA) constitutes a considerable proportion of fine particles in populated area, while there is a lack of understanding on its impact on climate. Using a data set from field observations in Beijing, we characterize the variations of COA in fine particulate matter (PM) and its effect on aerosols hygroscopicity and cloud condensation nuclei (CCN) activity. The observed mass concentrations of COA from two campaigns of winter 2016 and summer 2017 were $5.5 \pm 5.6 \mu\text{g m}^{-3}$ and $1.9 \pm 2.1 \mu\text{g m}^{-3}$, respectively, corresponding to mass fraction of COA to PM₁ and total OA of $8\% \pm 9\%$ and $17\% \pm 13\%$ in winter, $10\% \pm 9\%$ and $19\% \pm 13\%$ in summer. The strong COA sources are evidenced by apparent peak values in mass concentrations at lunch and dinner times. With increase of volume fraction of COA from $\sim 10\%$ during noncooking time to $\sim 40\%$ during dinner time, hygroscopic parameter of OA (κ_{org}) is decreased from ~ 0.21 to ~ 0.06 (corresponding to a decrease of overall hygroscopic parameter of aerosols, κ , from ~ 0.25 to ~ 0.20), showing a critical role of COA in altering aerosols hygroscopicity. Further evaluation shows that the decrease in aerosols hygroscopicity caused by COA will reduce its CCN activity significantly (characterized by critical supersaturation, S_c , increasing from $\sim 0.25\%$ – 0.5% to $\sim 0.4\%$ – 0.7%). The current circumstance, which presents no apparent downward trends of COA in Beijing during last decades but much greater levels of COA in China than those in other regions around the world, suggests the great significance to account for the effect of COA on regional climate in models.

1. Introduction

Cooking emission is a major source of fine particulate matter (PM) and organic aerosols (OA) in urban atmosphere (Abdullahi et al., 2013; Buonanno et al., 2009; Reyes-Villegas et al., 2018), generating great effects on both human health and air quality. It has been reported that emissions from cooking activities have resulted in the death of millions of people annually, according to the report from World Health Organization (<https://www.who.int/airpollution/household/en/>) (Y. He et al., 2019).

The composition of cooking aerosol, which depends on the ingredients of food materials and cooking style, varies largely in the atmosphere. Several typical tracers, such as alkanes, dicarboxylic acids, fatty acids, sterols, etc., have been used to characterize cooking source related aerosols (Abdullahi et al., 2013). In China, it has been found that the main component from cooking emission is usually C₆–C₂₄ fatty acid with midlong carbon chains (L.-Y. He et al., 2004), therefore, cooking aerosols may have a large surface area (Abdullahi et al., 2013). Organic carbon (OC) emissions ($1.9 \times 10^4 \text{ mg year}^{-1}$) from residential (indicated by cooking activities) are much higher than those emitted from transportation ($1.5 \times 10^3 \text{ mg year}^{-1}$) in urban Beijing, according to inventory of Multiresolution Emission Inventory for China (MEIC) (F. Liu et al., 2015). A very high emission rate of toxic equivalent from cooking sources was also revealed by C.-T. Li et al. (2003).

High mass concentrations of cooking source related organic aerosols (COA) have been measured in populated urban regions. For example, the higher mass concentration of COA ($6.6 \mu\text{g m}^{-3}$) than the hydrocarbon OA (HOA, $5.8 \mu\text{g m}^{-3}$) has been obtained in Beijing (Y. L. Sun et al., 2013). The COA has also been found to account for higher fraction of OA than traffic-related HOA in Lanzhou (J. Xu et al., 2014). Moreover, it is found that the photochemical products from oxidation of volatile organic compounds (VOCs) can condense

on the COA to form secondary organic aerosol (SOA) in urban areas (T. Liu et al., 2018; Roe et al., 2005). Therefore, the characterization of COA is of great significance to elucidate its effect on regional air quality and climate. Many studies have explored different methods to quantify COA, including positive matrix factorization (PMF) analysis, receptor models. COA and other OA (e.g., traffic OA, primarily composed by HOA) can be well separated by PMF method, owing to their distinct mass spectrum characteristics. In addition, the diurnal variations of COA are usually characterized by two distinct peaks during meal time (Hu et al., 2016; X.-F. Huang et al., 2010; P. Xu et al., 2017).

The hygroscopicity of fine particles, which can impact air quality and climate by affecting their CCN activity, the radiative forcing, and visibility (Hudson & Clarke, 1992; Qi et al., 2018), highly depends on the chemical composition, atmospheric transformation, and types and emissions of gas precursors under diverse environments (Fan et al., 2020; Zhang, Li, et al., 2014; Zhang, Wang, et al., 2017). Usually, the COA is nonhydrophilic with hygroscopic parameter (κ) value of 0, while the experimental study revealed that the hygroscopicity of the COA enhanced greatly after photochemical aging, and the mass fraction of soluble COA was doubled, from 24% to 55% (Y. Li et al., 2018). Another earlier experimental study showed that the degree of oxidation of COA enhanced markedly after photochemical aging (Kaltsonoudis et al., 2017). Also, Y. Li et al. (2018) reported that aged COA is more hygroscopic and CCN active than the fresh one. Due to the strong emissions in populated urban area, its aging and the variations of the hygroscopicity and CCN activity of those freshly emitted COA would be expected to be more complex.

In this study, based on two field measurements in the winter of 2016 and summer of 2017 in urban Beijing, we characterize the levels and variations of COA in fine aerosol particles and its effect on aerosols hygroscopicity and CCN activity. The study is structured as follows. The methods are presented in Section 2. The time series of COA are shown in Section 3.1. The diurnal variations of COA are shown in Section 3.2. The impact of COA on hygroscopicity of aerosol are investigated in Section 3.3. The sensitivity of aerosol CCN activity to variations in κ and κ_{org} are examined in Section 3.4. Implications and conclusions are given in Section 4.

2. Materials and Methods

We conducted the field measurements at the campus of Institute of Atmospheric Physics (IAP). The site is located in the central area of urban Beijing, and there are some restaurants around the site. The sampling site is influenced by multiple factors, including cooking emissions from nearby restaurants, vehicle emissions from road traffic. Therefore, cooking emissions can be important at the site, and the cooking activities impacts the diurnal patterns of COA. The observation at the site can represent typical urban background (regional characteristics), and also can well capture local impacts (Sun, Du, et al., 2016). As shown in Figure 1, the mass concentration of COA is with both large spikes and baselines. Two campaigns were conducted in winter of 2016 (from 18 November to 15 December) and summer of 2017 (from 25 May to 18 June), respectively. One of the key instruments deployed in two campaigns is aerodyne high-resolution time-of-flight aerosol mass spectrometer (HR-ToF-AMS), which is used to measure the chemical composition of nonrefractory size-resolved fine PM with a sampling height of approximately 4 m from ground. The measured NR-PM₁ species include organics (Org), sulfate (SO₄), nitrate (NO₃), ammonium (NH₄), and chloride (Chl). Mean particle number size distributions of PM₁ species measured during the campaigns are shown in Figure S1. More detailed description of the field measurements and instruments can be found in W. Xu et al. (2015). BC was measured in two campaigns using a light absorption with an aethalometer (AE33, Magee Scientific Corp., Drinovec et al., 2015). AMS PMF with PMF algorithm (v4.2) method was applied to identify COA factor (P. Xu et al., 2017). The detailed operation of PMF has been described by W. Xu et al. (2015), W. Xu et al. (2019) and J. Liu et al. (2021). In addition to the COA factor, three other primary OA factors, HOA, fossil fuel-related OA (FFOA), and biomass burning OA (BBOA), are also separated for analysis.

The hygroscopicity of fine aerosol particles is measured by a Hygroscopic Tandem Differential Mobility Analyzer (HTDMA) system. The first DMA was used to select the size of quasimonodisperse particles to obtain the D_{dry} . Before get into the DMA, the particles were dried to a relative humidity (RH) < 20% by a Nafion dryer. The second DMA was used to measure the grown size of the humidified quasimonodisperse

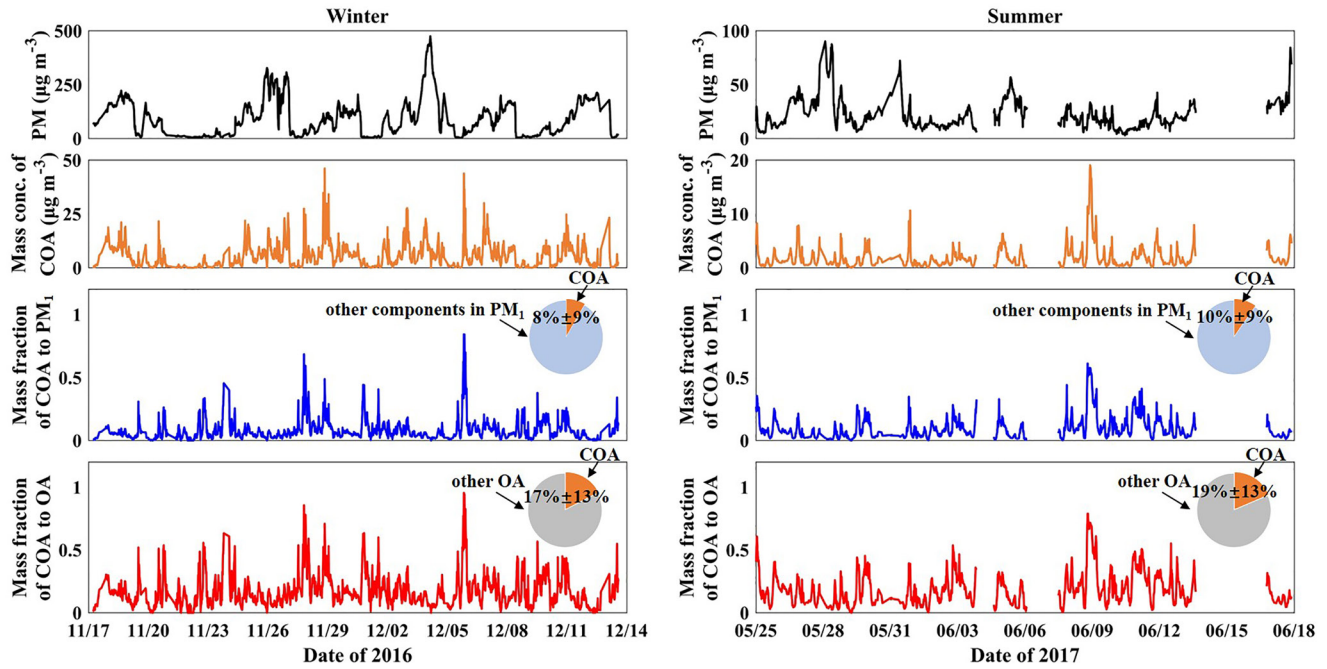


Figure 1. Time series of mass concentration of PM₁, cooking organic aerosol (COA) and mass fraction of COA to PM₁ and total OA in winter (left) and summer (right). The pie charts embedded in the figure represent the campaign mean mass fraction of COA (orange), other components (blue) to PM₁, and mean mass fraction of other OA (gray) to total OA. OA, organic aerosol; PM, particulate matter.

particles to obtain the D_{wet} . The hygroscopic growth factor (G_f) is derived by the ratio of $D_{\text{wet}}/D_{\text{dry}}$. A Nafion humidifier was used to humidify the quasimonodisperse particles to the specified relative humidity (90%). RH was calibrated regularly with ammonium sulfate during the campaign. The first DMA and a water-based condensation particle counter (WCPC, model 3787, TSI Inc.) can be connected directly to measure the 10–400 nm particle number size distribution (PNSD). In this study, the selected dry diameters were 40, 80, 110, 150, and 200 nm, respectively, according to previous studies (Fan et al., 2020; Wang, Zhang, et al., 2017). In this study, we obtained bulk hygroscopicity of OA (κ_{org}) by averaging value of κ of particles with different diameters. We used mean κ to calculate the overall hygroscopicity of OA based on the mixing rule with the size-resolved aerosol chemical compositions measured by AMS (Petters & Kreidenweis, 2007) (SI: Methods). More detailed calculation methods of κ and κ_{org} are given in J. Liu et al. (2021). The volume of COA were calculated according to its mass concentration and density (1.0 g cm^{-3}). And the volume fraction of COA (ε_{COA}) can be obtained by dividing the volume of COA by the volume of total OA,

$$\varepsilon_{\text{COA}} = \frac{m_{\text{COA}}}{\rho_{\text{COA}} V_{\text{total-OA}}} \quad (1)$$

where m_{COA} is the mass concentration of COA. ρ_{COA} is the density of COA. $V_{\text{total-OA}}$ is the volume of total OA.

And we express the CCN activity of aerosols as critical supersaturation (S_c). According to the κ -Köhler theory, the supersaturation ratio corresponding to the critical particle size can be interpreted as the S_c corresponding to the particle size. For $\kappa > 0.1$, the particle critical supersaturation with specific particle size (D_p) can be calculated by the following expressions (Petters & Kreidenweis, 2007),

$$\kappa = \frac{4A}{27D_p^3 S_c^2} \quad (2)$$

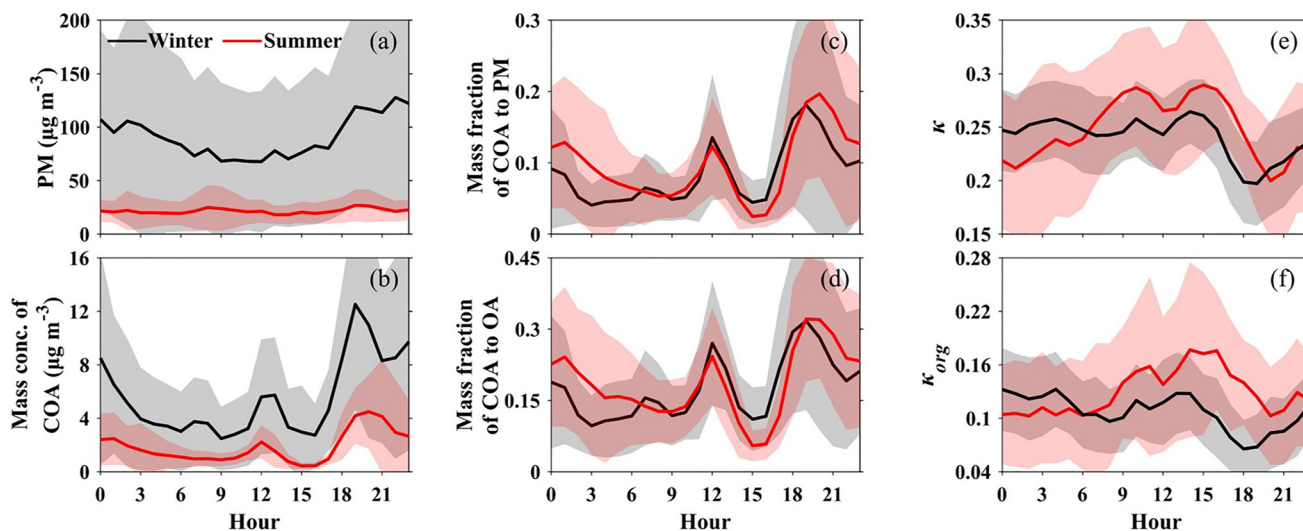


Figure 2. Averaged diurnal patterns in mass concentration of PM₁ (a) and cooking organic aerosol (COA) (b), mass fraction of COA to PM₁ (c), mass fraction of COA to total OA (d), bulk κ (e) and κ_{org} (f) in winter (black lines) and summer (red lines). The shade regions denote the standard deviation ($\pm 1\sigma$). OA, organic aerosol; PM, particulate matter.

$$A = \frac{4\sigma_{s/a}M_w}{RT\rho_w} \quad (3)$$

where κ is the overall hygroscopicity of aerosols. S_c is the particle critical supersaturation. D_p is the dry diameter of the particles, $\sigma_{s/a}$ is the surface tension of the solution/air (assumed to be the surface tension of pure water, $\sigma_{s/a} = 0.0728 \text{ N m}^{-2}$), R is the universal gas constant, T is the absolute temperature, M_w is the molecular weight of water, and ρ_w is the density of water.

3. Results and Discussion

3.1. Time Series

The COA spectrum in winters of 2016 shows a high ratio of m/z 55/57 (~ 2.2), and the O/C of COA is ~ 0.16 in winter of 2016 (W. Xu et al., 2019). The COA factor in summer of 2017 was obtained by the same method as in winter of 2016. And the COA is correlated with $\text{C}_6\text{H}_{10}\text{O}^+$, which is a tracer for cooking emissions (W. Xu et al., 2019). The time series of mass concentration of PM₁ and COA, mass fraction of COA to PM₁, and mass fraction of COA to total OA during the campaign are presented in Figure 1. The mass concentrations of PM₁ and COA both in the summer and winter were observed presenting large fluctuations, which should be closely associated with the variations of meteorological conditions, emission sources and rapid formation of fine particles, etc. The PM₁ and COA mass concentration was observed during winter with campaign average values of $90.4 \pm 83.3 \mu\text{g m}^{-3}$ and $5.5 \pm 5.6 \mu\text{g m}^{-3}$, corresponding to mass fraction of COA to PM₁ and OA of $8\% \pm 9\%$ and $17\% \pm 13\%$ respectively. In summer, the mass concentration of PM₁ and COA show much lower ambient levels, with campaign averages of $21.7 \pm 13.3 \mu\text{g m}^{-3}$ and $1.9 \pm 2.1 \mu\text{g m}^{-3}$, respectively, but with similar mass fraction and the COA constituted a considerable fraction of PM₁ mass ($10\% \pm 9\%$) and OA ($19\% \pm 13\%$). Occasionally, the mass concentration of COA can be as high as $50 \mu\text{g m}^{-3}$ (with mass fraction of more than 90% to total OA), indicating that emission from cooking activity is a primary source of PM₁ in urban Beijing.

3.2. Diurnal Variations

As shown in Figure 2, the PM₁ mass concentration in winter and summer exhibited distinct diurnal variations (Figure 2a). In winter, the diurnal variation of PM₁ mass concentration presented a shallow “U” shape, which is low in the daytime and high during nighttime, reflecting the influence due to changes of planetary

boundary layer (PBL) in winter. On the contrary, the mass concentration of PM₁ shows insignificant diurnal variation in summer. This is likely due to that the stronger photochemical processing yields more secondary aerosols during daytime in summer (Y. L. Sun et al., 2013), which offsets the dilution effect of the PBL during daytime. The diurnal cycles of COA in winter and summer both show two notable peaks corresponding to lunch (11:00–14:00 local time, LT) and dinner (18:00–21:00 LT) times. Such pattern is presented at the sites in other cities of China (Elser et al., 2016; X.-F. Huang et al., 2010; Wang, Huang, et al., 2017) and reflects the strong impacts from local cooking emissions. As addressed above, higher mass concentration of COA in winter than that in summer is observed, which is mainly caused by distinct characteristics in the PBL heights, since the cooking activity may not change much between summer and winter (Duan et al., 2020, Figure S2). The diurnal patterns of mass fraction of COA to PM₁ and total OA are generally in accordance with the diurnal cycles of COA mass concentration in winter and summer (Figures 2c and 2d). The mass fraction of COA to OA can be as high as 27% and 32% during the lunch and dinner times (Figure 2d), respectively, corresponding to mass fraction of COA to PM₁ of 14% and 20% (Figure 2c). The COA has been found to account for higher fraction of OA than traffic-related HOA (Y. L. Sun et al., 2013, Figure S3). This again suggests that COA is a primary local source of primary organic aerosol (POA) that may take critical role in regional climate. The diurnal cycles of both the κ and κ_{org} are similar between winter and summer (Figures 2e and 2f), but showing slightly higher in summer than that in winter. The higher κ and κ_{org} in summer is probably enhanced by stronger photochemical processing in summer particularly during daytime (J. Liu et al., 2021). In addition, a remarkable decline in the κ and κ_{org} at dinner time and a slight decrease at lunch time are observed, indicating the impact of COA on aerosols hygroscopicity (Figures 2e and 2f).

3.3. Impact of COA on Hygroscopicity of the Fine Aerosol Particles

To elucidate the effect of COA on hygroscopicity of OA, the dependence of κ_{org} on volume fraction of COA is further examined (Figure 3). Our results show that, both in the winter and summer, the κ_{org} is decreased linearly from ~ 0.15 (~ 0.21 in winter) to ~ 0.06 (0.09 in winter) with increasing of the volume fraction of COA from $\sim 10\%$ to 40% . Linear correlations are also obtained in winter ($\kappa_{\text{org}} = -0.27 \epsilon\text{COA} + 0.17$, $R^2 = 0.51$) and summer ($\kappa_{\text{org}} = -0.27 \epsilon\text{COA} + 0.21$, $R^2 = 0.88$). The largest volume fraction of COA is observed during dinner time (as high as $\sim 40\%$), which corresponds to the smallest κ_{org} of OA (denoted by the blue dots in Figure 3a), indicating a large impact of the COA on the hygroscopicity of organic aerosols. The volume fraction of COA at noncooking time is smaller, with mean ϵCOA of 16% in winter and 19% in summer, with elevated κ_{org} and κ of 0.11 ± 0.04 and 0.25 ± 0.04 in winter, and 0.13 ± 0.07 and 0.25 ± 0.07 in summer, respectively. Note that although the volume fraction of COA increased at lunch time, the mean κ_{org} and κ did not show apparent decrease by comparing with the values at noncooking time (Figure 3b). This has been demonstrated that the summer strong photochemical oxidation around noon time yields more highly oxidized OA which is more water-soluble and enhances the overall hygroscopicity of aerosols (J. Liu et al., 2021). In addition, the water solubility of COA is probably enhanced after photochemical aging by exposure to ultraviolet (Y. Li et al., 2018). The dependence of κ_{org} on other POA factors (i.e., FFOA, BBOA, and HOA) are further examined to explore the effect of other primary emissions on the hygroscopicity of OA (Figure 4), particularly given that the evening traffic rush hours may coincide with the dinner time. This has been indicated by the small elevations in the diurnal variations of the mass concentrations of the other POA factors (FFOA, BBOA, and HOA) during dinner time (Figures 4a and 4d). However, the κ_{org} does not show obvious dependence on the volume fraction of the FFOA and HOA (Figures 4b and 4e). A dependence of the κ_{org} on ϵBBOA is shown, exhibiting an increase in the value of κ_{org} with increase of ϵBBOA (Figure 4c). The results demonstrate that the decline in hygroscopicity of aerosols is primarily due to the strengthened emission of COA during dinner time in urban Beijing. In other words, the emissions of COA takes critical role in altering the water uptake capacity of aerosols, especially at mealtime in metropolis.

3.4. Sensitivity of Aerosol CCN Activity to Variations in κ and κ_{org}

To further study the effect of the strong COA emissions on the CCN activity, a sensitivity of aerosol CCN activity (denoted as S_c) to variations in κ and κ_{org} has been done based on κ -Köhler theory (Koehler, 1936) (Figure 5). As just indicated by the κ -Köhler equation, the result shows that, variations in D_p and κ (or κ_{org}) played an important role in modifying aerosols CCN activity. The changes of S_c are more sensitive to

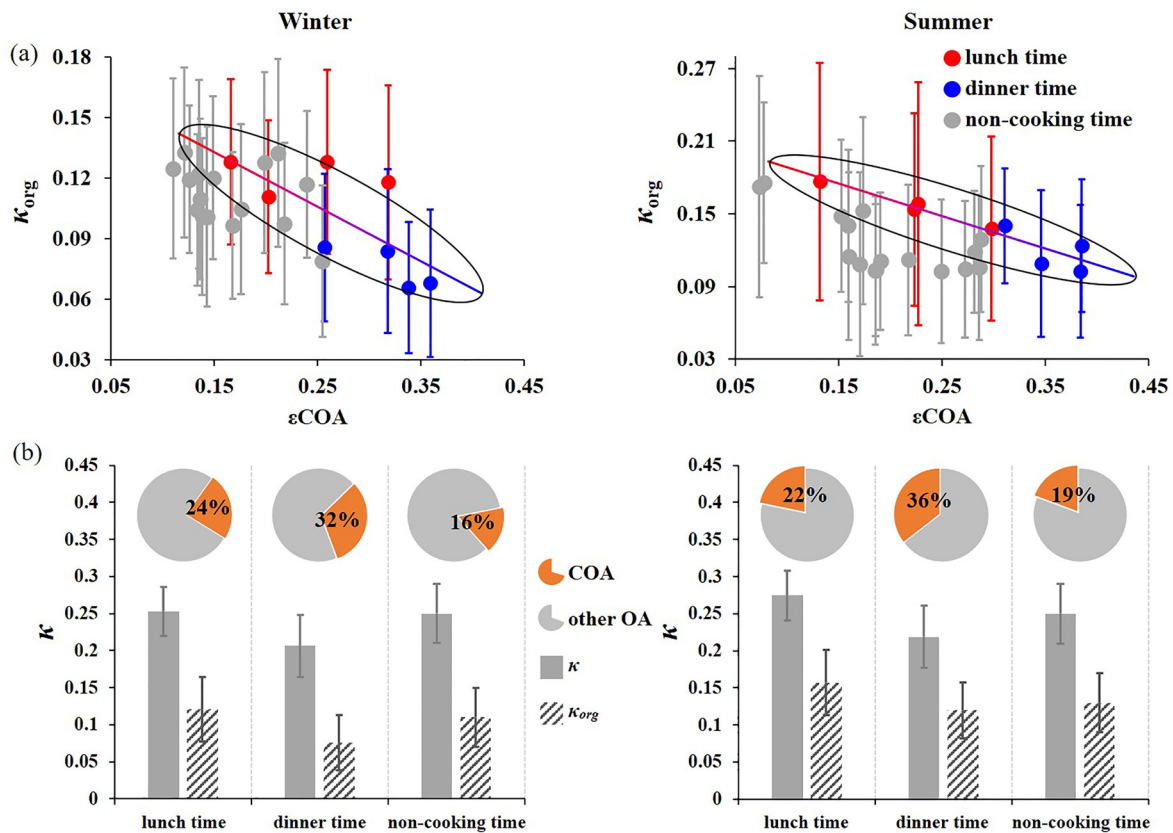


Figure 3. The dependence of κ_{org} on volume fraction of cooking organic aerosol (COA) (ϵ_{COA}) on lunch time (11:00–14:00 local time, LT) and dinner time (18:00–21:00 LT). The lines represent the linear fitting of κ_{org} and ϵ_{COA} . Ellipses are the auxiliary of linear fitting (a); Statistics mean value of κ , κ_{org} , volume fraction of COA (orange part of pie chart), and other OA (gray part of pie chart) during lunch, dinner, and noncooking time (b). The error bars represent $\pm 1\sigma$.

changes of aerosols hygroscopicity for small particles. The effect due to changes in aerosol hygroscopicity on S_c gradually weakened with the increase of particle size. For particles diameters of >200 nm, S_c required for activation to CCN increased slightly as the hygroscopicity of aerosol slacken. This is because the curvature effect is no longer dominant for large particles (Koehler, 1936; F. Zhang et al., 2019). For a given particle size, variations in S_c reflect the impacts of changes in hygroscopicity of aerosol. According to our observation, the PNSD of COA during the two campaigns in urban Beijing peaked between 40 and 80 nm (Figure S4). In Figure 5, it shows that, with the decrease of aerosol hygroscopicity (κ_{org} decreased from ~ 0.21 to ~ 0.06) caused by COA, the required S_c to activate 50 nm particles (COA dominated size) increased from $\sim 0.55\%$ to $\sim 0.75\%$, reflecting that the CCN activity was depressed significantly due to the strong COA emissions. In general, the decrease of water uptake capacity of aerosols caused by increase of COA emissions will reduce the aerosol CCN activity greatly, with the required S_c to activate the ambient fine particles increased from ~ 0.3 – 0.5% to ~ 0.4 – 0.7% . Our results suggest that fresh emitted COA during mealtimes reduce the hygroscopicity of aerosols by varying the composition of aerosols, considerably affecting the ability of aerosols to serve as CCN. Our results imply the great significance of the COA to regional air quality and climate in populated urban areas, although it is not the primary component of OA and PM_{10} (Figures 1 and S3).

4. Implications and Conclusions

Emissions from cooking activities are a major source of urban primary particulate matter. From a review of field observations of ambient COA, we present that COA is a considerable component of OA in urban areas around the world (Figure 6). Globally, it shows that the fraction of COA in OA is 10%–30% (with mean value of $\sim 20\%$) across the world (Figure 6a). However, owing to the traditional cooking habits in China, much higher mean COA mass concentrations ($\sim 6.41 \mu\text{g m}^{-3}$) have been observed in most of the megacities

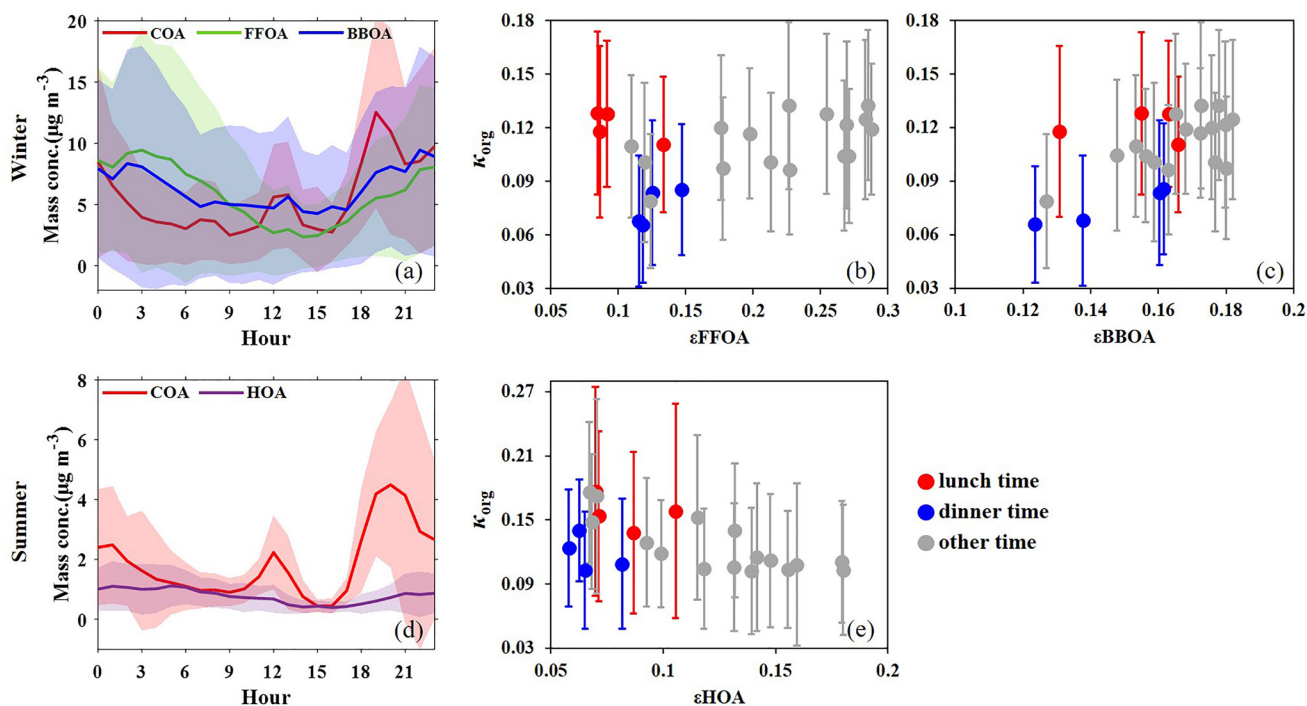


Figure 4. Average diurnal cycles of mass concentrations of primary organic aerosol (POA) factors in winter of 2016 (a) and summer of 2017 (d). The shade regions denote the standard deviation ($\pm 1\sigma$). The dependence of κ_{org} on volume fraction of FFOA (b), BBOA (c), and HOA (e) on lunch time (11:00–14:00 local time, LT) and dinner time (18:00–21:00 LT). The error bars represent $\pm 1\sigma$. BBOA, biomass burning OA; FFOA, fossil fuel-related OA; HOA, hydrocarbon OA; OA, organic aerosol.

in China than those in other regions, such as North America ($\sim 1.39 \mu\text{g m}^{-3}$) and Europe ($\sim 2.23 \mu\text{g m}^{-3}$) (Figure 6b). The COA levels observed by this study from our field campaigns in the winter of 2016 and summer of 2017 in urban Beijing are basically within the range of the previously reported results at other sites in China (Figure 6c). The mass concentrations of COA can be as high as up to 20–60 $\mu\text{g m}^{-3}$ in some cities (e.g., Beijing, Lanzhou, and Xi'an) in China, highlighting the critical role of COA in determine the levels of ambient fine particles and its effects on regional climate.

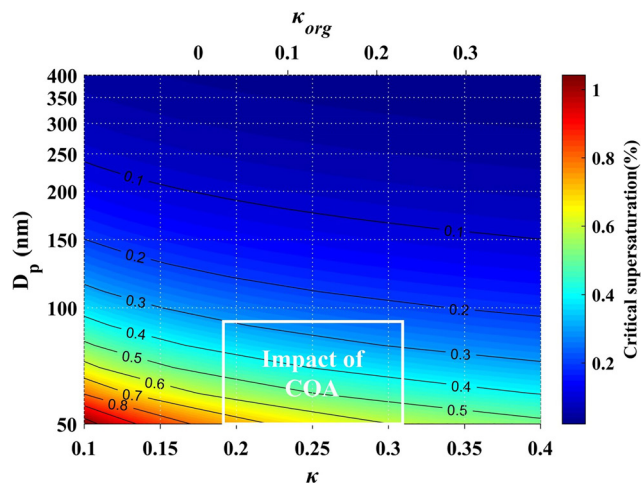


Figure 5. Sensitivity of S_c to the variations in κ and κ_{org} . The white box shows the zone that is impacted due to changes of κ and κ_{org} by the increase or decrease of fraction in cooking organic aerosol (COA) during the campaigns in urban Beijing.

By linking the COA emissions to aerosol particles hygroscopicity, we have shown that, with increase of volume fraction of COA from $\sim 10\%$ during noncooking time (background condition) to $\sim 40\%$ during dinner time, hygroscopic parameter of OA has been decreased from ~ 0.21 to ~ 0.06 (κ decreasing from ~ 0.25 to ~ 0.20), demonstrating the significant role of the COA sources in altering aerosols hygroscopicity in populated urban atmosphere. Further evaluation shows that the decrease in hygroscopicity of aerosols caused by COA will reduce the aerosol CCN activity markedly (S_c increased from $\sim 0.25\%$ – 0.5% to $\sim 0.4\%$ – 0.7%) for the ambient fine particles. The current circumstance, which presents no apparent downward trends of COA in urban atmosphere during last decades but much higher levels in ambient COA concentrations in China than those in other regions around the world (as shown in Figure 6), suggests the great significance to accurate parameterizing the effect of COA on regional air pollution and climate in models. In addition, due to the limitation of the PMF analysis, the information of the oxidation degree of the COA is not available in this study. However, it has been shown that the primary aerosols experienced rapid aging and secondary conversion in urban Beijing (Ren et al., 2018), it is likely that the freshly emitted hydrophobic COA become hygroscopic OA or oxidized COA, which can be serve as CCN.

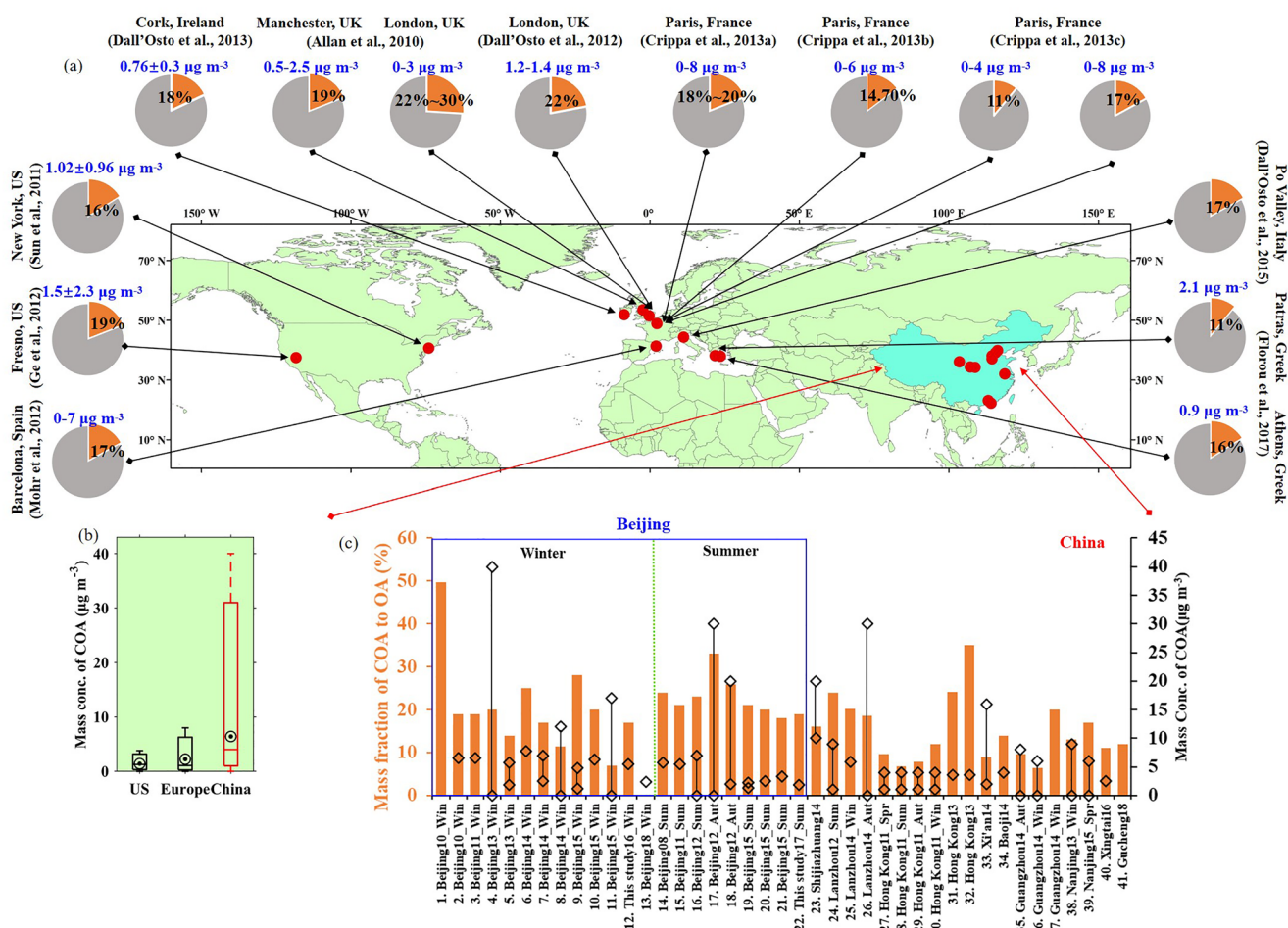


Figure 6. Summary of ambient observed cooking organic aerosol (COA) from literatures. (a) The mass concentration of COA and its mass fraction to OA around the world (Allan et al., 2010; Crippa, Canonaco, et al., 2013; Crippa, DeCarlo, et al., 2013; Crippa, El Haddad, et al., 2013; Dall'Osto and Harrison, 2012; Dall'Osto et al., 2013; Dall'Osto et al., 2015; Florou et al., 2017; Ge et al., 2012; Mohr et al., 2012; Y.-L. Sun et al., 2011); (b) The mean mass concentration of COA in North America, Europe and China; (c) Observations at sites in China. The black diamonds and orange columns are mass concentration of COA and its mass fraction to OA respectively. The references, Reference 1–Reference 41, are as follows: 1. Q. Liu et al., 2011; 2, 15. Hu et al., 2016; 3. Sun et al., 2013; 4. Zhang, Sun, et al., 2014; 5. Jiang et al., 2015; 6. W. Xu et al., 2019; 7, 11. J. K. Zhang et al., 2016; 8, 33. Elser et al., 2016; 9. Zhou et al., 2018; 10, 21. Duan et al., 2020; 12, 22. This study; 13. J. Li et al., 2019; 14. Huang et al., 2010; 16, 18. Zhang, Wang, et al., 2015; 17. P. Xu et al., 2017; 19. H. Li et al., 2016; 20. J. Li et al., 2020; 23. R.-J. Huang et al., 2019; 24. J. Xu et al., 2014; 25. J. Xu et al., 2016; 26. Zhang, Zhang, et al., 2017; 27–30. Y. J. Li et al., 2015; 31. Sun, Lee, et al., 2016; 32. Lee et al., 2015; 34. Wang, Huang, et al., 2017; 35, 36. Qin et al., 2017; 37. Lan et al., 2018; 38. Zhang, Tang, et al., 2015; 39. Wang et al., 2016; 40. Y. Zhang et al., 2018; 41. Kuang et al., 2020.

Therefore, a further study warrants to be done in future by considering the atmospheric chemical and physical processes of COA in the atmosphere.

Conflict of Interest

The authors declare no competing financial interest.

Data Availability Statement

All data needed to evaluate the conclusions in the study is available on <https://data.mendeley.com/datasets/v9jz9k2whb/1> or from the corresponding author upon request (fang.zhang@bnu.edu.cn).

Acknowledgments

This work was supported by the National Natural Science Foundation of China (Grants 41975174, 41675141), and the National Basic Research Program of China (2017YFC1501702).

References

- Abdullahi, K. L., Delgado-Saborit, J. M., & Harrison, R. M. (2013). Emissions and indoor concentrations of particulate matter and its specific chemical components from cooking: A review. *Atmospheric Environment*, *71*, 260–294. <https://doi.org/10.1016/j.atmosenv.2013.01.061>
- Allan, J. D., Williams, P. I., Morgan, W. T., Martin, C. L., Flynn, M. J., Lee, J., et al. (2010). Contributions from transport, solid fuel burning and cooking to primary organic aerosols in two UK cities. *Atmospheric Chemistry and Physics*, *10*, 647–668. <https://doi.org/10.5194/acp-10-647-2010>
- Buonanno, G., Morawska, L., & Stabile, L. (2009). Particle emission factors during cooking activities. *Atmospheric Environment*, *43*, 3235–3242. <https://doi.org/10.1016/j.atmosenv.2009.03.044>
- Crippa, M., Canonaco, F., Slowik, J. G., El Haddad, I., DeCarlo, P. F., Mohr, C., et al. (2013a). Primary and secondary organic aerosol origin by combined gas-particle phase source apportionment. *Atmospheric Chemistry and Physics*, *13*, 8411–8426. <https://doi.org/10.5194/acp-13-8411-2013>
- Crippa, M., DeCarlo, P. F., Slowik, J. G., Mohr, C., Heringa, M. F., Chirico, R., et al. (2013c). Wintertime aerosol chemical composition and source apportionment of the organic fraction in the metropolitan area of Paris. *Atmospheric Chemistry and Physics*, *13*, 961–981. <https://doi.org/10.5194/acp-13-961-2013>
- Crippa, M., El Haddad, I., Slowik, J. G., DeCarlo, P. F., Mohr, C., Heringa, M. F., et al. (2013b). Identification of marine and continental aerosol sources in Paris using high resolution aerosol mass spectrometry. *Journal of Geophysical Research: Atmospheres*, *118*, 1950–1963. <https://doi.org/10.1002/jgrd.50151>
- Dall'Osto, M., & Harrison, R. M. (2012). Urban organic aerosols measured by single particle mass spectrometry in the megacity of London. *Atmospheric Chemistry and Physics*, *12*, 4127–4142. <https://doi.org/10.5194/acp-12-4127-2012>
- Dall'Osto, M., Ovadnevaite, J., Ceburnis, D., Martin, D., Healy, R. M., O'Connor, I. P., et al. (2013). Characterization of urban aerosol in Cork city (Ireland) using aerosol mass spectrometry. *Atmospheric Chemistry and Physics*, *13*, 4997–5015. <https://doi.org/10.5194/acp-13-4997-2013>
- Dall'Osto, M., Paglione, M., Decesari, S., Facchini, M. C., O'Dowd, C., Plass-Dueller, C., & Harrison, R. M. (2015). On the origin of ams “cooking organic aerosol” at a rural site. *Environmental Science & Technology*, *49*, 13964–13972. <https://doi.org/10.1021/acs.est.5b02922>
- Drinovec, L., Močnik, G., Zotter, P., Prévôt, A. S. H., Ruckstuhl, C., Coz, E., et al. (2015). The “dual-spot” aethalometer: An improved measurement of aerosol black carbon with real-time loading compensation. *Atmospheric Measurement Techniques*, *8*, 1965–1979. <https://doi.org/10.5194/amt-8-1965-2015>
- Duan, J., Huang, R.-J., Li, Y., Chen, Q., Zheng, Y., Chen, Y., et al. (2020). Summertime and wintertime atmospheric processes of secondary aerosol in Beijing. *Atmospheric Chemistry and Physics*, *20*, 3793–3807. <https://doi.org/10.5194/acp-20-3793-2020>
- Elser, M., Huang, R.-J., Wolf, R., Slowik, J. G., Wang, Q., Canonaco, F., et al. (2016). New insights into PM_{2.5} chemical composition and sources in two major cities in China during extreme haze events using aerosol mass spectrometry. *Atmospheric Chemistry and Physics*, *16*, 3207–3225. <https://doi.org/10.5194/acp-16-3207-2016>
- Fan, X., Liu, J., Zhang, F., Chen, L., Collins, D., Xu, W., et al. (2020). Contrasting size-resolved hygroscopicity of fine particles derived by HTDMA and HR-ToF-AMS measurements between summer and winter in Beijing: The impacts of aerosol aging and local emissions. *Atmospheric Chemistry and Physics*, *20*, 915–929. <https://doi.org/10.5194/acp-20-915-2020>
- Florou, K., Papanastasiou, D. K., Pikridas, M., Kaltsonoudis, C., Louvaris, E., Gkatzelis, G. I., et al. (2017). The contribution of wood burning and other pollution sources to wintertime organic aerosol levels in two Greek cities. *Atmospheric Chemistry and Physics*, *17*, 3145–3163. <https://doi.org/10.5194/acp-17-3145-2017>
- Ge, X., Setyan, A., Sun, Y., & Zhang, Q. (2012). Primary and secondary organic aerosols in Fresno, California during wintertime: Results from high resolution aerosol mass spectrometry. *Journal of Geophysical Research*, *117*. <https://doi.org/10.1029/2012jd018026>
- He, L.-Y., Hu, M., Huang, X.-F., Yu, B.-D., Zhang, Y.-H., & Liu, D.-Q. (2004). Measurement of emissions of fine particulate organic matter from Chinese cooking. *Atmospheric Environment*, *38*, 6557–6564. <https://doi.org/10.1016/j.atmosenv.2004.08.034>
- He, Y., Sun, Y., Wang, Q., Zhou, W., Xu, W., Zhang, Y., et al. (2019). A black carbon-tracer method for estimating cooking organic aerosol from aerosol mass spectrometer measurements. *Geophysical Research Letters*, *46*, 8474–8483. <https://doi.org/10.1029/2019gl084092>
- Huang, R.-J., Wang, Y., Cao, J., Lin, C., Duan, J., Chen, Q., et al. (2019). Primary emissions versus secondary formation of fine particulate matter in the most polluted city (Shijiazhuang) in North China. *Atmospheric Chemistry and Physics*, *19*, 2283–2298. <https://doi.org/10.5194/acp-19-2283-2019>
- Huang, X.-F., He, L.-Y., Hu, M., Canagaratna, M. R., Sun, Y., Zhang, Q., et al. (2010). Highly time-resolved chemical characterization of atmospheric submicron particles during 2008 Beijing olympic games using an aerodyne high-resolution aerosol mass spectrometer. *Atmospheric Chemistry and Physics*, *10*, 8933–8945. <https://doi.org/10.5194/acp-10-8933-2010>
- Hudson, J. G., & Clarke, A. D. (1992). Aerosol and cloud condensation nuclei measurements in the Kuwait plume. *Journal of Geophysical Research*, *97*, 14533–14536. <https://doi.org/10.1029/92jd00800>
- Hu, W., Hu, M., Hu, W., Jimenez, J. L., Yuan, B., Chen, W., et al. (2016). Chemical composition, sources, and aging process of submicron aerosols in Beijing: Contrast between summer and winter. *Journal of Geophysical Research: Atmospheres*, *121*, 1955–1977. <https://doi.org/10.1002/2015jd024020>
- Jiang, Q., Sun, Y. L., Wang, Z., & Yin, Y. (2015). Aerosol composition and sources during the Chinese Spring Festival: Fireworks, secondary aerosol, and holiday effects. *Atmospheric Chemistry and Physics*, *15*, 6023–6034. <https://doi.org/10.5194/acp-15-6023-2015>
- Kaltsonoudis, C., Kostenidou, E., Louvaris, E., Psichoudaki, M., Tsiligiannis, E., Florou, K., et al. (2017). Characterization of fresh and aged organic aerosol emissions from meat charbroiling. *Atmospheric Chemistry and Physics*, *17*, 7143–7155. <https://doi.org/10.5194/acp-17-7143-2017>
- Koehler, H. (1936). The nucleus in and growth of hygroscopic droplets. *Transactions of the Faraday Society*, *32*, 1152–1161. <https://doi.org/10.1039/TF9363201152>
- Kuang, Y., He, Y., Xu, W., Yuan, B., Zhang, G., Ma, Z., et al. (2020). Photochemical aqueous-phase reactions induce rapid daytime formation of oxygenated organic aerosol on the North China Plain. *Environmental Science & Technology*, *54*, 3849–3860. <https://doi.org/10.1021/acs.est.9b06836>
- Lan, Z., Zhang, B., Huang, X., Zhu, Q., Yuan, J., Zeng, L., et al. (2018). Source apportionment of PM_{2.5} light extinction in an urban atmosphere in China. *Journal of Environmental Sciences*, *63*, 277–284. <https://doi.org/10.1016/j.jes.2017.07.016>
- Lee, B. P., Li, Y. J., Yu, J. Z., Louie, P. K. K., & Chan, C. K. (2015). Characteristics of submicron particulate matter at the urban roadside in downtown Hong Kong-Overview of 4 months of continuous high-resolution aerosol mass spectrometer measurements. *Journal of Geophysical Research - D: Atmospheres*, *120*, 7040–7058. <https://doi.org/10.1002/2015jd023311>

- Li, C.-T., LinLee, Y.-C. W., Lee, W.-J., & Tsai, P.-J. (2003). Emission of polycyclic aromatic hydrocarbons and their carcinogenic potencies from cooking sources to the urban atmosphere. *Environmental Health Perspectives*, *111*, 483–487. <https://doi.org/10.1289/ehp.5518>
- Li, H., Zhang, Q., Duan, F., Zheng, B., & He, K. (2016). The “Parade Blue”: Effects of short-term emission control on aerosol chemistry. *Faraday Discussions*, *189*, 317–335. <https://doi.org/10.1039/c6fd00004e>
- Li, J., Liu, Z., Cao, L., Gao, W., Yan, Y., Mao, J., et al. (2019). Highly time-resolved chemical characterization and implications of regional transport for submicron aerosols in the North China Plain. *The Science of the Total Environment*, *705*, 135803. <https://doi.org/10.1016/j.scitotenv.2019.135803>
- Li, J., Liu, Z., Gao, W., Tang, G., Hu, B., Ma, Z., & Wang, Y. (2020). Insight into the formation and evolution of secondary organic aerosol in the megacity of Beijing, China. *Atmospheric Environment*, *220*, 117070. <https://doi.org/10.1016/j.atmosenv.2019.117070>
- Liu, F., Zhang, Q., Tong, D., Zheng, B., Li, M., Huo, H., et al. (2015). High-resolution inventory of technologies, activities, and emissions of coal-fired power plants in China from 1990 to 2010. *Atmospheric Chemistry and Physics*, *15*, 13299–13317. <https://doi.org/10.5194/acp-15-13299-2015>
- Liu, J., Zhang, F., Xu, W., Sun, Y., Chen, L., Li, S., et al. (2021). Hygroscopicity of organic aerosols linked to formation mechanisms. *Geophysical Research Letters*, *48*, e2020GL091683. <https://doi.org/10.1029/2020gl091683>
- Liu, Q., Sun, Y., Hu, B., Liu, Z., Akio, S., & Wang, Y. (2011). In situ measurement of PM1 organic aerosol in Beijing winter using a high-resolution aerosol mass spectrometer. *Chinese Science Bulletin*, *57*, 819–826. <https://doi.org/10.1007/s11434-011-4886-0>
- Liu, T., Wang, Z., Huang, D. D., Wang, X., & Chan, C. K. (2018). Significant production of secondary organic aerosol from emissions of heated cooking oils. *Environmental Science & Technology Letters*, *5*, 32–37. <https://doi.org/10.1021/acs.estlett.7b00530>
- Li, Y. J., Lee, B. P., Su, L., Fung, J. C. H., & Chan, C. K. (2015). Seasonal characteristics of fine particulate matter (PM) based on high-resolution time-of-flight aerosol mass spectrometric (HR-ToF-AMS) measurements at the HKUST Supersite in Hong Kong. *Atmospheric Chemistry and Physics*, *15*, 37–53. <https://doi.org/10.5194/acp-15-37-2015>
- Li, Y., Tasoglou, A., Liangou, A., Cain, K. P., Jahn, L., Gu, P., et al. (2018). Cloud condensation nuclei activity and hygroscopicity of fresh and aged cooking organic aerosol. *Atmospheric Environment*, *176*, 103–109. <https://doi.org/10.1016/j.atmosenv.2017.11.035>
- Mohr, C., DeCarlo, P. F., Heringa, M. F., Chirico, R., Slowik, J. G., Richter, R., et al. (2012). Identification and quantification of organic aerosol from cooking and other sources in Barcelona using aerosol mass spectrometer data. *Atmospheric Chemistry and Physics*, *12*, 1649–1665. <https://doi.org/10.5194/acp-12-1649-2012>
- Petters, M. D., & Kreidenweis, S. M. (2007). A single parameter representation of hygroscopic growth and cloud condensation nucleus activity. *Atmospheric Chemistry and Physics*, *7*, 1961–1971. <https://doi.org/10.5194/acp-7-1961-2007>
- Qin, Y. M., Tan, H. B., Li, Y. J., Schurman, M. I., Li, F., Canonaco, F., et al. (2017). Impacts of traffic emissions on atmospheric particulate nitrate and organics at a downwind site on the periphery of Guangzhou, China. *Atmospheric Chemistry and Physics*, *17*, 10245–10258. <https://doi.org/10.5194/acp-17-10245-2017>
- Qi, X., Sun, J., Zhang, L., Shen, X., Zhang, X., Zhang, Y., et al. (2018). Aerosol hygroscopicity during the haze red-alert period in December 2016 at a rural site of the North China Plain. *Journal of Meteorological Research*, *32*, 38–48. <https://doi.org/10.1007/s13351-018-7097-7>
- Ren, J., Zhang, F., Wang, Y., Collins, D., Fan, X., Jin, X., et al. (2018). Using different assumptions of aerosol mixing state and chemical composition to predict CCN concentrations based on field measurements in urban Beijing. *Atmospheric Chemistry and Physics*, *18*, 6907–6921. <https://doi.org/10.5194/acp-18-6907-2018>
- Reyes-Villegas, E., Bannan, T., Le Breton, M., Mehra, A., Priestley, M., Percival, C., et al. (2018). Online chemical characterization of food-cooking organic aerosols: Implications for source apportionment. *Environmental Science & Technology*, *52*, 5308–5318. <https://doi.org/10.1021/acs.est.7b06278>
- Roe, S. M., Spivey, M. D., Lindquist, H. C., Hemmer, P., & Huntley, R. (2005). *National emissions inventory for commercial cooking*. The U.S. Environmental Protection Agency, (EPA) Emission Factor and Inventory Group (EFIG).
- Sun, C., Lee, B. P., Huang, D., Jie Li, Y., Schurman, M. I., Louie, P. K. K., et al. (2016a). Continuous measurements at the urban roadside in an Asian megacity by Aerosol Chemical Speciation Monitor (ACSM): Particulate matter characteristics during fall and winter seasons in Hong Kong. *Atmospheric Chemistry and Physics*, *16*, 1713–1728. <https://doi.org/10.5194/acp-16-1713-2016>
- Sun, Y., Du, W., Fu, P., Wang, Q., Li, J., Ge, X., et al. (2016b). Primary and secondary aerosols in Beijing in winter: sources, variations and processes. *Atmospheric Chemistry and Physics*, *16*(13), 8309–8329. <https://doi.org/10.5194/acp-16-8309-2016>
- Sun, Y. L., Wang, Z. F., Fu, P. Q., Yang, T., Jiang, Q., Dong, H. B., et al. (2013). Aerosol composition, sources and processes during winter-time in Beijing, China. *Atmospheric Chemistry and Physics*, *13*, 4577–4592. <https://doi.org/10.5194/acp-13-4577-2013>
- Sun, Y.-L., Zhang, Q., Schwab, J. J., Demerjian, K. L., Chen, W.-N., Bae, M.-S., et al. (2011). Characterization of the sources and processes of organic and inorganic aerosols in New York city with a high-resolution time-of-flight aerosol mass spectrometer. *Atmospheric Chemistry and Physics*, *11*, 1581–1602. <https://doi.org/10.5194/acp-11-1581-2011>
- Wang, J., Ge, X., Chen, Y., Shen, Y., Zhang, Q., Sun, Y., et al. (2016). Highly time-resolved urban aerosol characteristics during springtime in Yangtze River Delta, China: Insights from soot particle aerosol mass spectrometry. *Atmospheric Chemistry and Physics*, *16*, 9109–9127. <https://doi.org/10.5194/acp-16-9109-2016>
- Wang, Y. C., Huang, R.-J., Ni, H. Y., Chen, Y., Wang, Q. Y., Li, G. H., et al. (2017b). Chemical composition, sources and secondary processes of aerosols in Baoji city of northwest China. *Atmospheric Environment*, *158*, 128–137. <https://doi.org/10.1016/j.atmosenv.2017.03.026>
- Wang, Y., Zhang, F., Li, Z., Tan, H., Xu, H., Ren, J., et al. (2017a). Enhanced hydrophobicity and volatility of submicron aerosols under severe emission control conditions in Beijing. *Atmospheric Chemistry and Physics*, *17*, 5239–5251. <https://doi.org/10.5194/acp-17-5239-2017>
- Xu, J., Shi, J., Zhang, Q., Ge, X., Canonaco, F., Prévôt, A. S. H., et al. (2016). Wintertime organic and inorganic aerosols in Lanzhou, China: Sources, processes, and comparison with the results during summer. *Atmospheric Chemistry and Physics*, *16*, 14937–14957. <https://doi.org/10.5194/acp-16-14937-2016>
- Xu, J., Zhang, Q., Chen, M., Ge, X., Ren, J., & Qin, D. (2014). Chemical composition, sources, and processes of urban aerosols during summertime in northwest China: Insights from high-resolution aerosol mass spectrometry. *Atmospheric Chemistry and Physics*, *14*, 12593–12611. <https://doi.org/10.5194/acp-14-12593-2014>
- Xu, P., Zhang, J., Ji, D., Liu, Z., Tang, G., Jiang, C., & Wang, Y. (2017). Characterization of submicron particles during autumn in Beijing, China. *Journal of Environmental Sciences*, *63*, 16–27. <https://doi.org/10.1016/j.jes.2017.03.036>
- Xu, W., Sun, Y., Chen, C., Du, W., Han, T., Wang, Q., et al. (2015). Aerosol composition, oxidation properties, and sources in Beijing: Results from the 2014 Asia-Pacific economic cooperation summit study. *Atmospheric Chemistry and Physics*, *15*, 13681–13698. <https://doi.org/10.5194/acp-15-13681-2015>
- Xu, W., Sun, Y., Wang, Q., Zhao, J., Wang, J., Ge, X., et al. (2019). Changes in aerosol chemistry from 2014 to 2016 in winter in Beijing: Insights from high-resolution aerosol mass spectrometry. *Journal of Geophysical Research - D: Atmospheres*, *124*, 1132–1147. <https://doi.org/10.1029/2018jd029245>

- Zhang, F., Li, Y., Li, Z., Sun, L., Li, R., Zhao, C., et al. (2014a). Aerosol hygroscopicity and cloud condensation nuclei activity during the AC3Exp campaign: Implications for cloud condensation nuclei parameterization. *Atmospheric Chemistry and Physics*, *14*, 13423–13437. <https://doi.org/10.5194/acp-14-13423-2014>
- Zhang, F., Ren, J., Fan, T., Chen, L., Xu, W., Sun, Y., et al. (2019). Significantly enhanced aerosol CCN activity and number concentrations by nucleation-initiated haze events: A case study in urban Beijing. *Journal of Geophysical Research: Atmospheres*, *124*, 14102–14113. <https://doi.org/10.1029/2019jd031457>
- Zhang, F., Wang, Y., Peng, J., Ren, J., Collins, D., Zhang, R., et al. (2017a). Uncertainty in predicting CCN activity of aged and primary aerosols. *Journal of Geophysical Research: Atmospheres*, *122*, 11723–11736. <https://doi.org/10.1002/2017jd027058>
- Zhang, J. K., Cheng, M. T., Ji, D. S., Liu, Z. R., Hu, B., Sun, Y., & Wang, Y. S. (2016). Characterization of submicron particles during biomass burning and coal combustion periods in Beijing, China. *The Science of the Total Environment*, *562*, 812–821. <https://doi.org/10.1016/j.scitotenv.2016.04.015>
- Zhang, J. K., Sun, Y., Liu, Z. R., Ji, D. S., Hu, B., Liu, Q., & Wang, Y. S. (2014b). Characterization of submicron aerosols during a month of serious pollution in Beijing, 2013. *Atmospheric Chemistry and Physics*, *14*, 2887–2903. <https://doi.org/10.5194/acp-14-2887-2014>
- Zhang, J., Wang, Y., Huang, X., Liu, Z., Ji, D., & Sun, Y. (2015a). Characterization of organic aerosols in Beijing using an aerodyne high-resolution aerosol mass spectrometer. *Advances in Atmospheric Sciences*, *32*, 877–888. <https://doi.org/10.1007/s00376-014-4153-9>
- Zhang, X., Zhang, Y., Sun, J., Yu, Y., Canonaco, F., Prévôt, A. S. H., & Li, G. (2017b). Chemical characterization of submicron aerosol particles during wintertime in a northwest city of China using an Aerodyne aerosol mass spectrometry. *Environmental Pollution*, *222*, 567–582. <https://doi.org/10.1016/j.envpol.2016.11.012>
- Zhang, Y., Du, W., Wang, Y., Wang, Q., Wang, H., Zheng, H., et al. (2018). Aerosol chemistry and particle growth events at an urban downwind site in North China Plain. *Atmospheric Chemistry and Physics*, *18*, 14637–14651. <https://doi.org/10.5194/acp-18-14637-2018>
- Zhang, Y., Tang, L., Yu, H., Wang, Z., Sun, Y., Qin, W., et al. (2015b). Chemical composition, sources and evolution processes of aerosol at an urban site in Yangtze River Delta, China during wintertime. *Atmospheric Environment*, *123*, 339–349. <https://doi.org/10.1016/j.atmosenv.2015.08.017>
- Zhou, W., Wang, Q., Zhao, X., Xu, W., Chen, C., Du, W., et al. (2018). Characterization and source apportionment of organic aerosol at 260 m on a meteorological tower in Beijing, China. *Atmospheric Chemistry and Physics*, *18*, 3951–3968. <https://doi.org/10.5194/acp-18-3951-2018>

Reference From the Supporting Information

- Gysel, M., McFiggans, G. B., & Coe, H. (2009). Inversion of tandem differential mobility analyser (TDMA) measurements. *Journal of Aerosol Science*, *40*, 134–151. <https://doi.org/10.1016/j.jaerosci.2008.07.013>